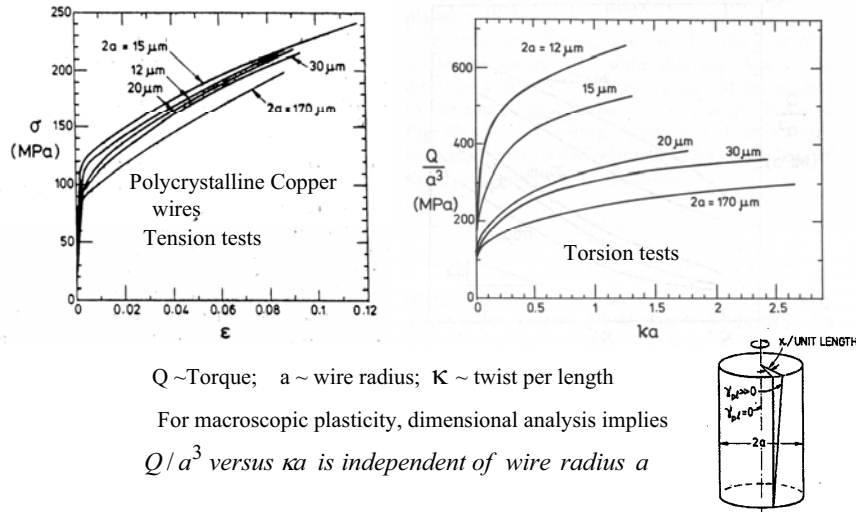


### MOTIVATION FOR STRAIN GRADIENT PLASTICITY:

The Size Effect in Wire Torsion (Fleck, Muller, Ashby & Hutch, 1994)



A strong size effect emerges for torsion (but NOT tension) of wires with diameters in the tens of microns

### Strain gradient plasticity: theory versus experiment

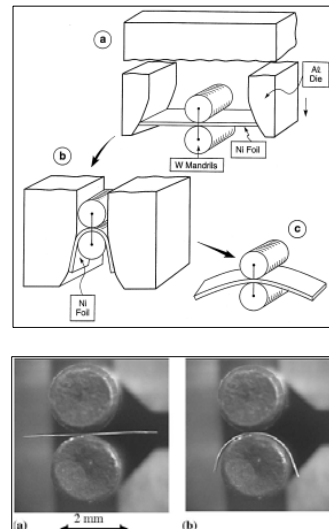
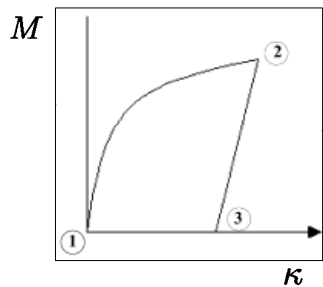
Norman A Fleck  
Cambridge University Engineering Dept.

#### Summary

- Review of experimental evidence for size effects
  - torsion, shear, bending, grain boundary roughening, indentation
- A flow theory with strain-gradient effects (Fleck-Willis, 2008)
  - with extremum principles, including the rigid, hardening limit
- Case studies:
  - predicted size effects for beams in bending and metallic foams
  - a layer in shear (compare with discrete dislocation simulations)

### Microbending tests

- The microbending of thin foils is a fundamental material test to underpin strain-gradient plasticity theories
- In the Stolken & Evans (1998) set up, a thin foil is bent over a circular cylindrical bar whose diameter sets the value of applied curvature; the moment is deduced from elastic spring back upon release:



Shrotriya et al. (2003)

### When are strain gradients significant? When strains vary over microns..

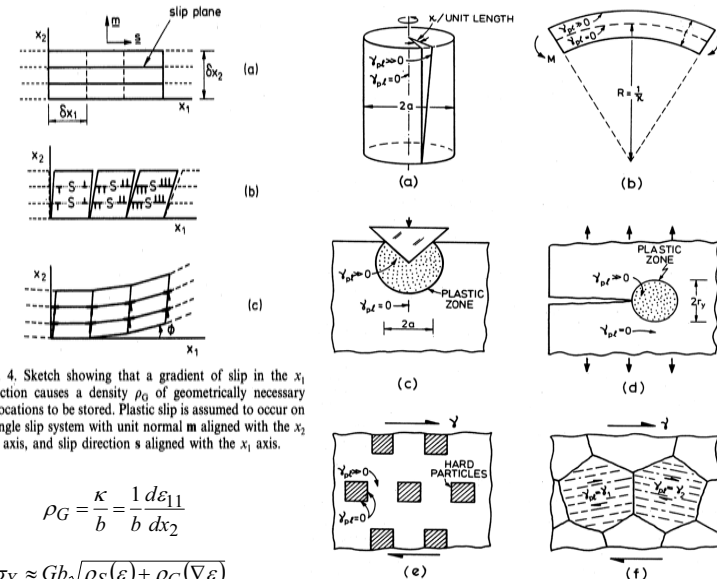


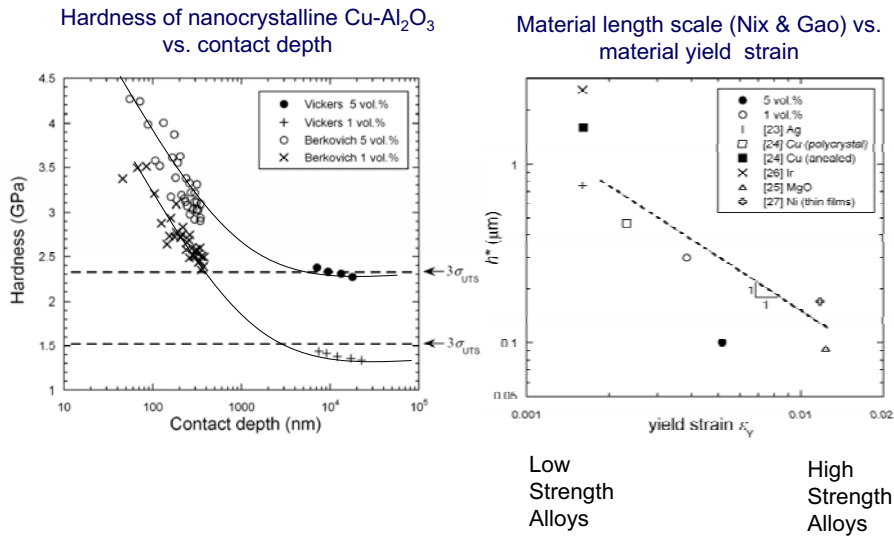
Fig. 4. Sketch showing that a gradient of slip in the  $x_1$  direction causes a density  $\rho_G$  of geometrically necessary dislocations to be stored. Plastic slip is assumed to occur on a single slip system with unit normal  $\mathbf{m}$  aligned with the  $x_2$  axis, and slip direction  $\mathbf{s}$  aligned with the  $x_1$  axis.

$$\rho_G = \frac{\kappa}{b} = \frac{1}{b} \frac{d\epsilon_{11}}{dx_2}$$

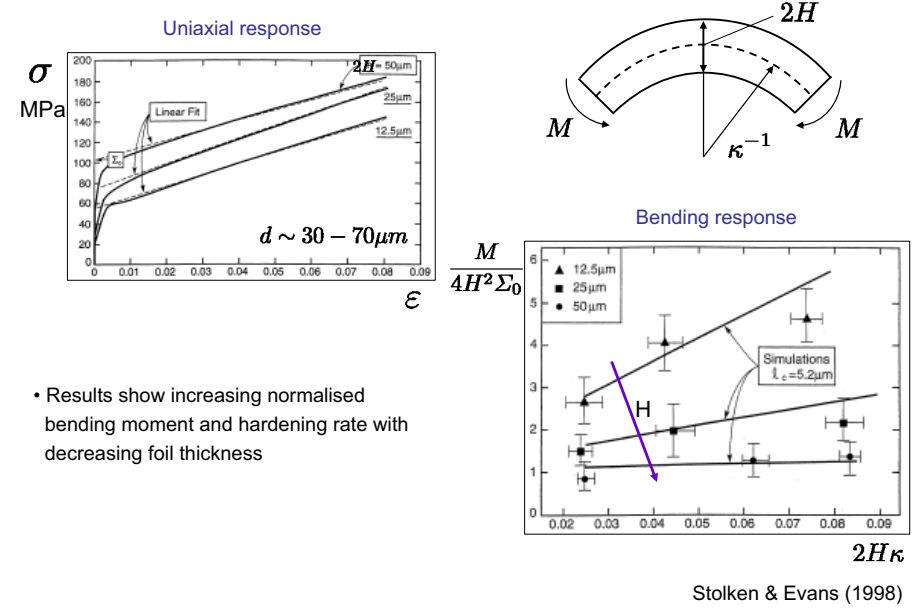
$$\sigma_Y \approx Gb\sqrt{\rho_S(\epsilon) + \rho_G(\nabla\epsilon)}$$

Fig. 1. Plastic strain gradients are caused by the geometry of deformation (a, b), by local boundary conditions (c, d) or by the microstructure itself (e, f).

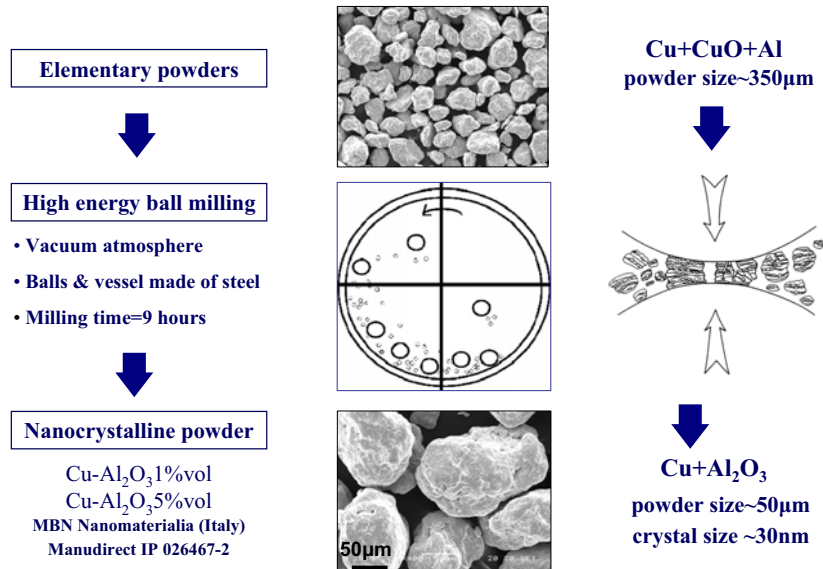
## Indentation size effect in nanocrystalline alloys



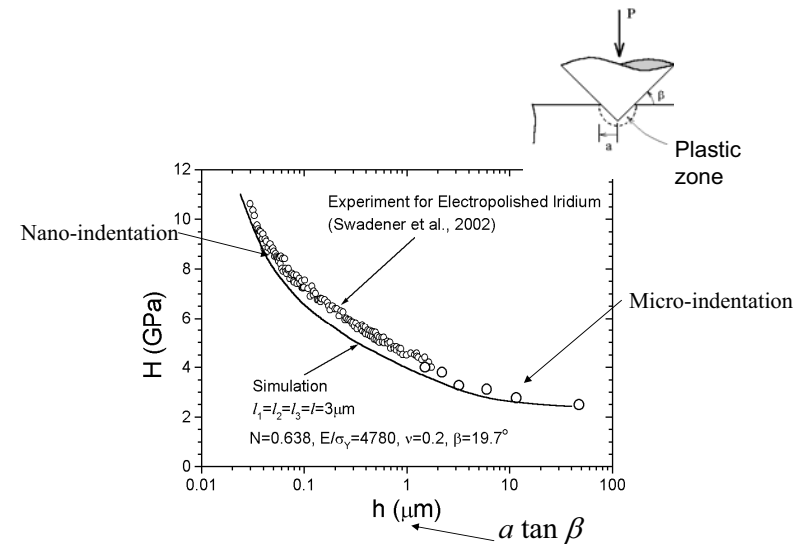
## Experimental results on Ni foils



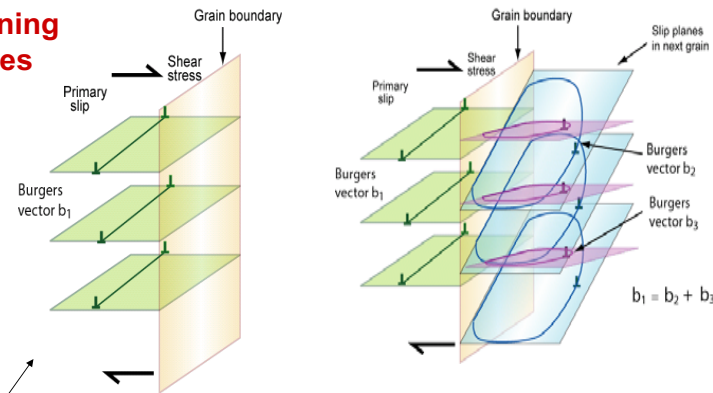
## Mechanical alloying



## Conical Indentation of Iridium By Swadener, George & Pharr (2002)



## Strengthening at interfaces

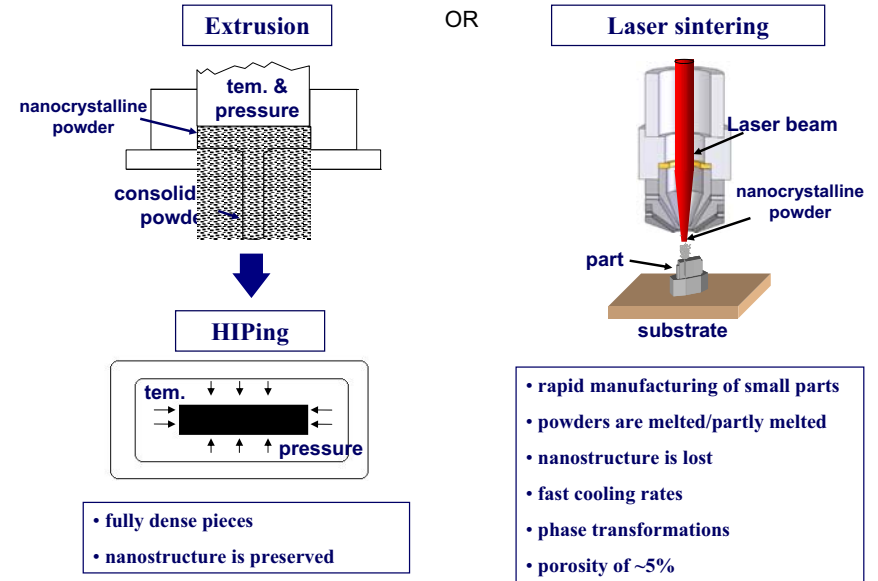


GNDs can accumulate at grain boundaries, with a jump in plastic strain, and give strengthening. (Usual interpretation)

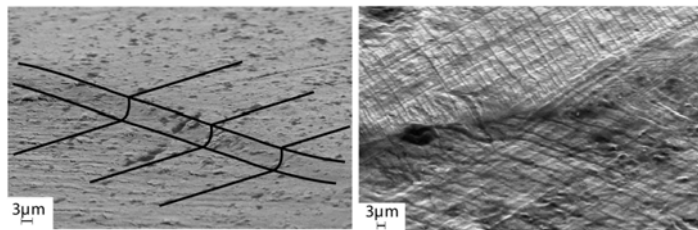
OR, Grain boundaries can act as obstacles without storage of GNDs, as shown here. There is no jump in plastic strain but grain boundary dislocations still accumulate and give strengthening.



## Consolidation



Plastic strain is almost continuous at interfaces, but they still lead to the Hall-Petch effect. SEM images of a grain boundary in aluminium sheet at a uniaxial strain of 10%. Grain size = 5mm, thickness = 1mm

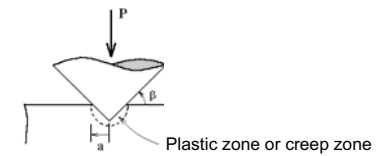
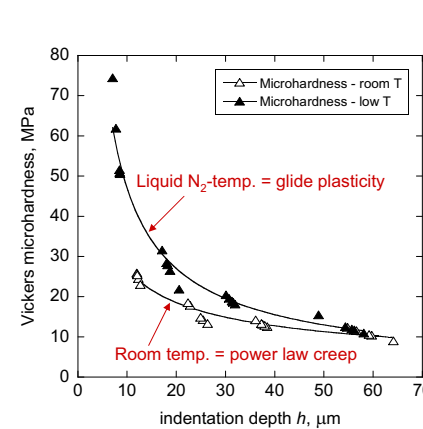


Local roughening at grain boundary

Multiple slip adjacent to grain boundary

Borg and Fleck (2007)

Size effects persist into the creep regime, and of similar magnitude !



Tests on Indium by Tagarielli-Fleck (2009)

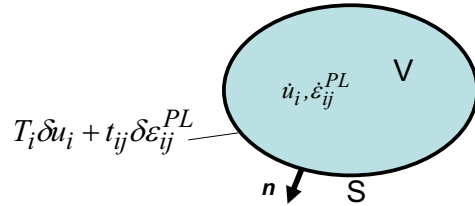
Indium is very soft and has a large internal material length scale.

## Elements of gradient plasticity theory (Gudmundson (2004); Fleck & Willis, 2008)

$u_i, \varepsilon_{ij}^{PL}$  are the basic kinematic quantities at each point  $x$

$$\varepsilon_{ij} = \frac{1}{2}(u_{i,j} + u_{j,i})$$

$$\varepsilon_{ij}^{EL} = \varepsilon_{ij} - \varepsilon_{ij}^{PL}$$



Neglect internal interfaces, and assume internal virtual work has elastic work and plastic dissipation:

$$\int_V \left\{ \sigma_{ij} \delta \varepsilon_{ij}^{EL} + Q_{ij} \delta \varepsilon_{ij}^{PL} + \tau_{ijk} \delta \varepsilon_{ij,k}^{PL} \right\} dV = \int_S \left\{ T_i \delta u_i + t_{ij} \delta \varepsilon_{ij}^{PL} \right\} dS$$

Hence:  $Q_{ij} - \tau_{ijk,k} - \sigma'_{ij} = 0$  and  $\sigma_{ij,j} = 0$

Take as constitutive law:  $\sigma_{ij} = L_{ijkl} (\varepsilon_{kl} - \varepsilon_{kl}^{PL})$

Need a constitutive law for  $Q$  and  $\tau$  in terms of plastic strain + its gradient...

## Interfaces disrupt the Voigt bound!

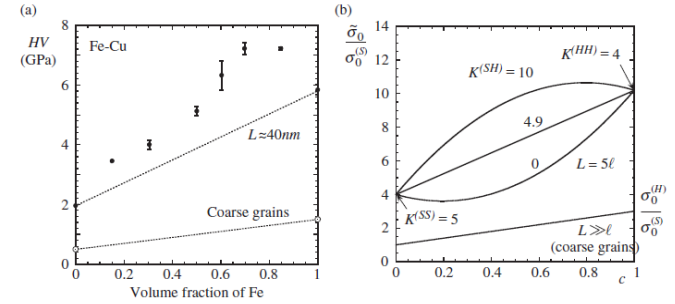
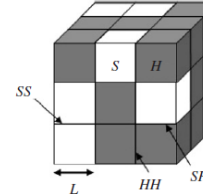


Figure 1. (a) Vickers hardness of Fe-Cu nanocrystalline composites ( $L \approx 40$  nm) versus the volume fraction of Fe, from [4]. (b) Elementary Voigt bounds for the effective strength of a two-phase composite with interfaces, as a function of volume fraction  $c$  of the hard phase.

Table 1. Idealized two-phase nanocrystalline material with interfaces.

component	strength	vol. fraction or surf. / vol. ratio
hard phase	$\sigma_0^{(H)}$	$c$
soft phase	$\sigma_0^{(S)}$	$1 - c$
hard-hard interfaces	$\kappa_c^{(HH)} \ell \sigma_0^{(H)}$	$(3/L) c^2$
soft-soft interfaces	$\kappa_c^{(SS)} \ell \sigma_0^{(S)}$	$(3/L)(1 - c)^2$
hard-soft interfaces	$\kappa_c^{(SH)} \ell \left( \sigma_0^{(S)} \sigma_0^{(H)} \right)^{1/2}$	$(3/L) 2c(1 - c)$



## Yield condition at a material point within V

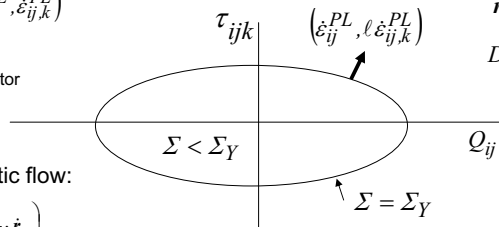
Define  $\dot{E}_P^2 = \dot{\varepsilon}_{ij}^{PL} \dot{\varepsilon}_{ij}^{PL} + \ell^2 \dot{\varepsilon}_{ij,k}^{PL} \dot{\varepsilon}_{ij,k}^{PL}$  and  $\Sigma^2 = Q_{ij} Q_{ij} + \ell^{-2} \tau_{ijk} \tau_{ijk}$

$(\dot{E}^P)^2 \equiv A_{IJ} \dot{e}_I \dot{e}_J$   $\Sigma^2 = D_{IJ} r_I r_J$  where

$\dot{e} = (\dot{e}_I) = (\dot{\varepsilon}_{ij}^{PL}, \dot{\varepsilon}_{ij,k}^{PL})$   $r = (r_I) = (Q_{ij}, \tau_{ijk})$

$D_{IJ} \equiv (A^{-1})_{IJ}$

15-dimensional vector

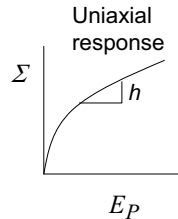


Associated plastic flow:

$$\dot{e} = \frac{1}{h} \frac{\partial \Sigma}{\partial r} \left( \frac{\partial \Sigma}{\partial r} \cdot \dot{r} \right)$$

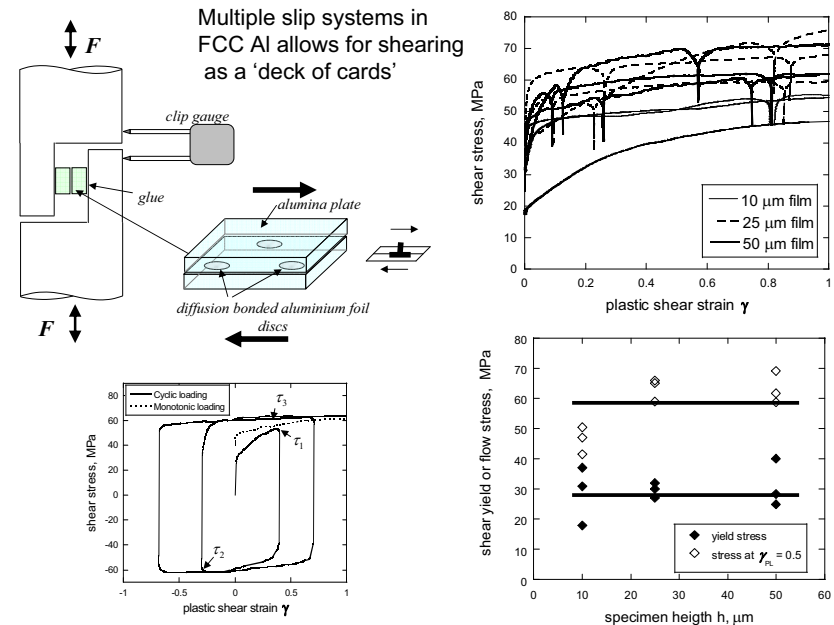
$$\dot{\varepsilon}_{ij}^{PL} = \frac{\dot{\Sigma}}{h(E_P)} \frac{\partial \Sigma}{\partial Q_{ij}} \quad \text{and} \quad \ell \dot{\varepsilon}_{ij,k}^{PL} = \frac{\dot{\Sigma}}{h(E_P)} \frac{\partial \Sigma}{\partial \tau_{ijk}}$$

Plastic work rate =  $Q_{ij} \dot{\varepsilon}_{ij}^{PL} + \tau_{ijk} \dot{\varepsilon}_{ij,k}^{PL} = \Sigma \dot{E}_P \geq 0$

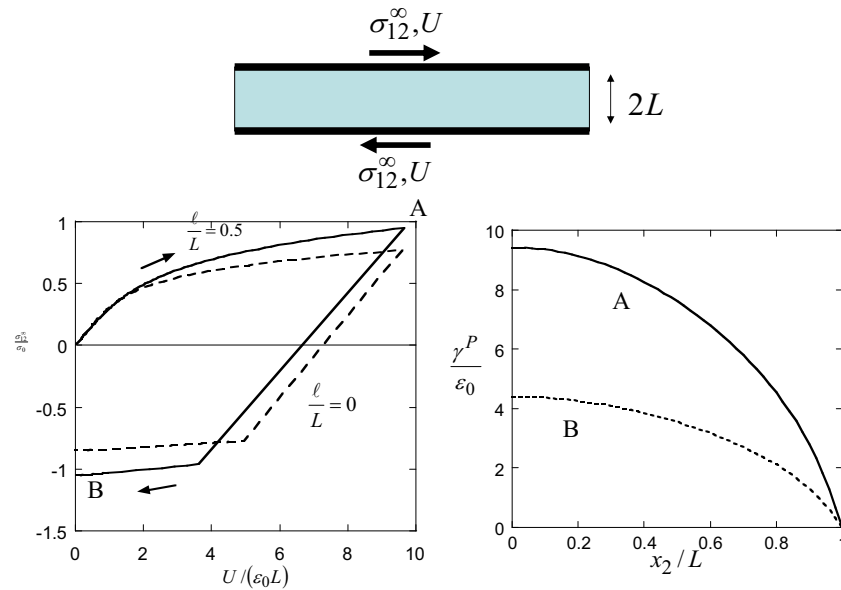


Minimum principles exist to solve the rate problem.

## Possible size effects in a sandwiched aluminium film under shear

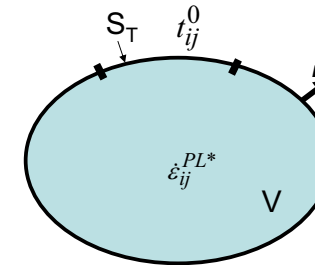


## Case Study: shear of a thin layer



## Minimum Principle I: determination of plastic strain rate field

Assume a trial field  $\dot{\epsilon}_{ij}^{PL*}$



The actual solution is: 
$$H = \inf_{\dot{\epsilon}_{ij}^{PL*}} \int_V \{ \Sigma_Y \dot{E}^{P*} - \sigma'_{ij} \dot{\epsilon}_{ij}^{PL*} \} dV - \int_{S_T} \{ t_{ij}^0 \dot{\epsilon}_{ij}^{PL*} \} dS$$

The solution for  $r$  is unique, and plastic strain rate is unique up to a multiplier  $\dot{\lambda}$

$$\dot{\epsilon}_{ij}^{PL}(\mathbf{x}) = \dot{\lambda} \hat{\epsilon}_{ij}(\mathbf{x}) \quad \text{where} \quad \frac{1}{V_a} \int_{V_a} \{ \hat{\epsilon}_{ij} \hat{\epsilon}_{ij} \} dV_a = 1$$

## Rigid-hardening solid

Deep in the plastic range, we can neglect elasticity. Then,  $\dot{\epsilon}_{ij}^{PL} \equiv \frac{1}{2}(\dot{u}_{i,j} + \dot{u}_{j,i})$

**Minimum Principle I** becomes: 
$$H = \inf_{\dot{u}_i^*} \int_V \{ \Sigma_Y \dot{E}^{P*} \} dV - \int_{S_T} \{ \bar{T}_i^0 \dot{u}_i^* + R_i^0 (D\dot{u}_i^*) \} dS$$

For a conventional solid, Hill (1948): 
$$H = \inf_{\dot{u}_i^*} \int_V \{ \sigma_Y \dot{\epsilon}_{eff}^* \} dV - \int_{S_T} \{ \bar{T}_i^0 \dot{u}_i^* \} dS$$

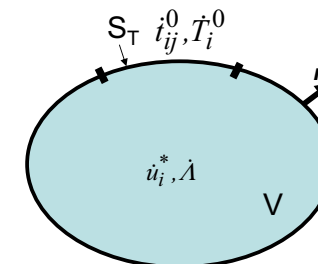
**Minimum Principle II** becomes: minimise  $J$  where

$$J(\dot{\lambda}^*) = \frac{1}{2} \int_V \{ H \dot{\epsilon}_{eff}^{P*2} \} dV - \int_{S_T} \{ \bar{T}_i^0 \dot{u}_i^* + R_i^0 (D\dot{u}_i^*) \} dS$$

Compare for conventional solid, Hill (1956): 
$$J(\dot{\lambda}^*) = \frac{1}{2} \int_V \{ H \dot{\epsilon}_{eff}^{*2} \} dV - \int_{S_T} \{ \bar{T}_i^0 \dot{u}_i^* \} dS$$

## Minimum Principle II: determination of velocity field and $\dot{\lambda}$

Assume  $\hat{\epsilon}_{ij}(\mathbf{x})$  is known.



The actual solution minimises:

$$J(\dot{u}_i^*, \dot{\lambda}^*) = \frac{1}{2} \int_V \{ L_{ijkl} (\dot{\epsilon}_{ij}^* - \dot{\epsilon}_{ij}^{PL*}) (\dot{\epsilon}_{kl}^* - \dot{\epsilon}_{kl}^{PL*}) + H \dot{\epsilon}_{eff}^{P*2} \} dV - \int_{S_T} \{ \bar{T}_i^0 \dot{u}_i^* + t_{ij}^0 \dot{\epsilon}_{ij}^{P*} \} dS$$

Unique solution for  $\dot{u}_i(\mathbf{x})$  and  $\dot{\lambda}$

$$\dot{\epsilon}_{ij}^{PL}(\mathbf{x}) = \dot{\lambda} \hat{\epsilon}_{ij}(\mathbf{x})$$

## Strain-gradient plasticity analysis

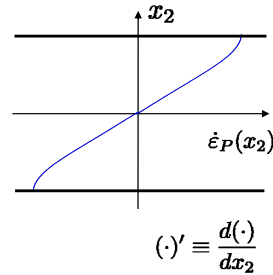
- The "effective" strain rate is

$$\dot{E}_P = \sqrt{\frac{2}{3} \left( \dot{\varepsilon}_{ij}^{PL} \dot{\varepsilon}_{ij}^{PL} + \ell^2 \dot{\varepsilon}_{ij,k}^{PL} \dot{\varepsilon}_{ij,k}^{PL} \right)} = \sqrt{\dot{\varepsilon}_P^2 + (\ell \dot{\varepsilon}'_P)^2}$$

- Decompose

$$\dot{\varepsilon}_P(x_2) = \dot{\lambda} \hat{\varepsilon}_P(x_2), \quad \frac{1}{H} \int_0^H \dot{\varepsilon}_P^2(x_2) dx_2 = 1, \quad \dot{\lambda} \geq 0$$

"magnitude" "unit" distribution



- First minimum principle:** given the current state, minimize

$$\min_{\hat{\varepsilon}_P} \int_0^H \left[ \sigma_y(E_P) \hat{E}_P - \frac{\sqrt{3}}{2} \sigma_{11} \hat{\varepsilon}_P \right] dx_2 \quad (\text{numerically})$$

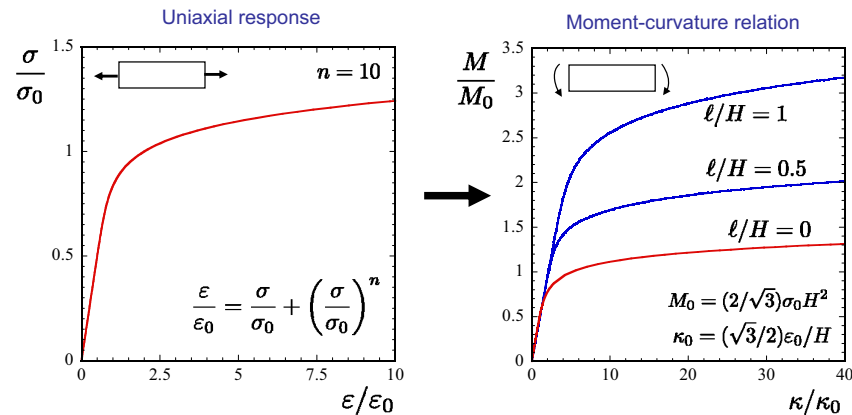
- Second minimum principle:** given the current state and the unit distribution, minimize

$$\min_{\dot{\lambda}} \int_0^H \left[ E \left( \frac{2}{\sqrt{3}} \dot{\kappa} x_2 - \dot{\lambda} \hat{\varepsilon}_P \right)^2 + h(E_P) \dot{\lambda}^2 \hat{E}_P^2 \right] dx_2 \quad (\text{analytically})$$



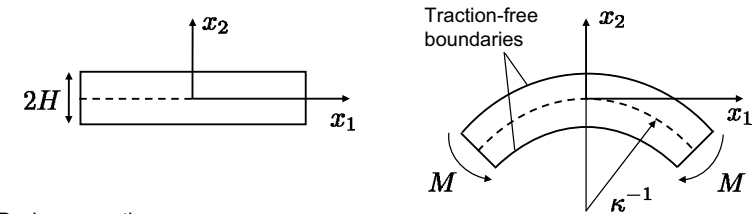
Application to the bending of thin foils

## Elasto-plastic foils



- predictions show increasing yield moment & hardening rate with decreasing foil thickness
- bending moment is elevated by a factor of ~2.5 when  $(\ell/H)$  goes from 0 to 1

## Strain-gradient plasticity analysis



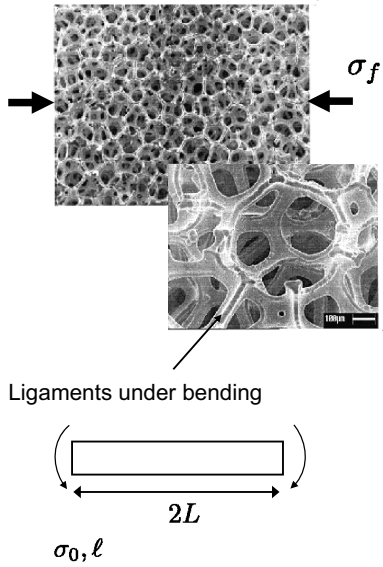
- Basic assumptions:

- material is homogeneous, isotropic and incompressible; dissipative plasticity
- curvature is applied via displacement boundary conditions at the ends of the foil
- traction-free top and bottom boundaries
- infinitesimal deformations; plane strain conditions
- total and plastic strain-rate fields:

$$\dot{\varepsilon}_{11} = -\dot{\varepsilon}_{22} = \dot{\kappa} x_2, \quad \dot{\varepsilon}_{12} = 0, \quad \dot{\varepsilon}_{i3} = 0$$

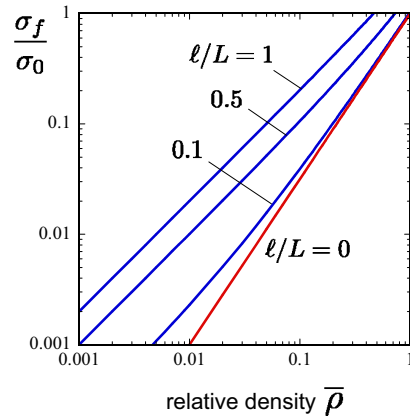
$$\dot{\varepsilon}_{11}^{PL} = -\dot{\varepsilon}_{22}^{PL} = (\sqrt{3}/2) \dot{\varepsilon}_P(x_2), \quad \dot{\varepsilon}_{12}^{PL} = 0, \quad \dot{\varepsilon}_{i3}^{PL} = 0$$

## Application to open-cell metallic foams

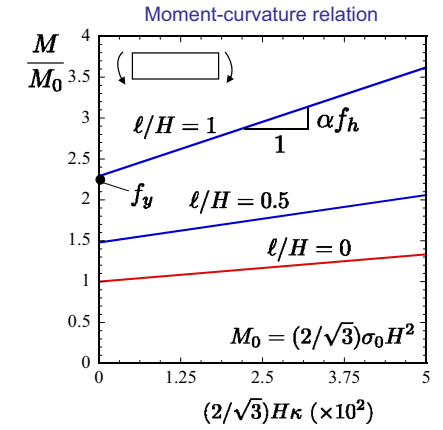
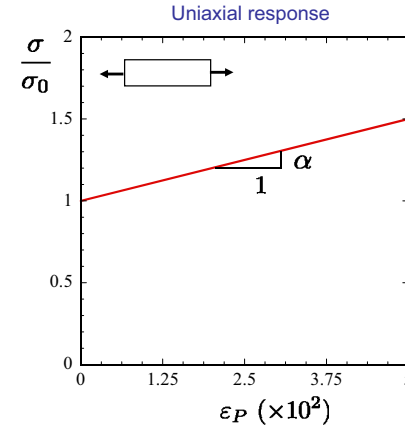


$$\frac{\sigma_f}{\sigma_0} \sim f_y \left( \frac{\ell}{L} \frac{1}{\bar{\rho}^{1/2}} \right) \bar{\rho}^{3/2}$$

$$f_y(\beta) = \sqrt{1 + \beta^2} + \beta^2 \sinh^{-1}(\beta^{-1})$$



## Rigid-plastic approximation – Linear hardening

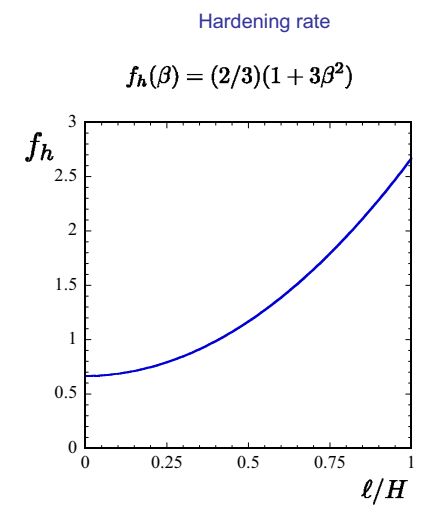
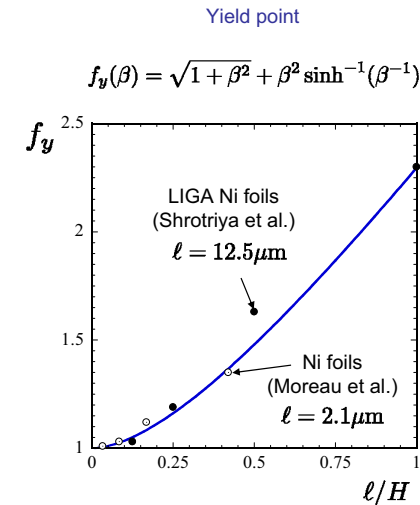


• closed-form moment-curvature relation:

$$\frac{M}{M_0} = f_y(\ell/H) + \alpha f_h(\ell/H) \frac{2}{\sqrt{3}} H\kappa$$

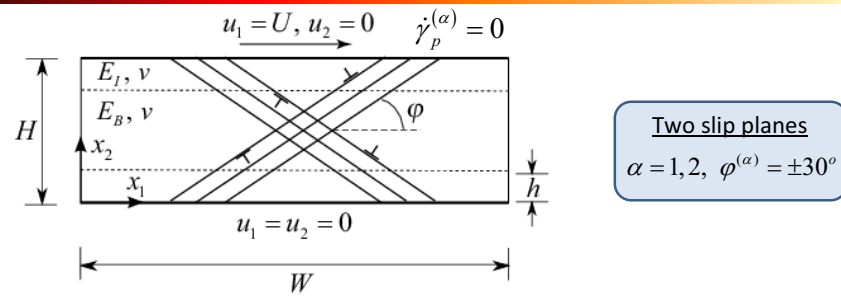
The sandwiched sheared single  
crystal problem

## Rigid-plastic approximation – Linear hardening



- closed-form expressions for power-law hardening also available
- these expressions provide a simple means of extracting material length scales from data

# Model Problem of a prototypical single crystal



$H$  : height of the crystal

$h$  : height of the interface

$E_B$  : Young's modulus of bulk

$E_I$  : Young's modulus of interface

$\nu$  : Poisson ratio

□ Subscripts:  $B$  for the bulk crystal &  $I$  for the interface

Slip direction vector

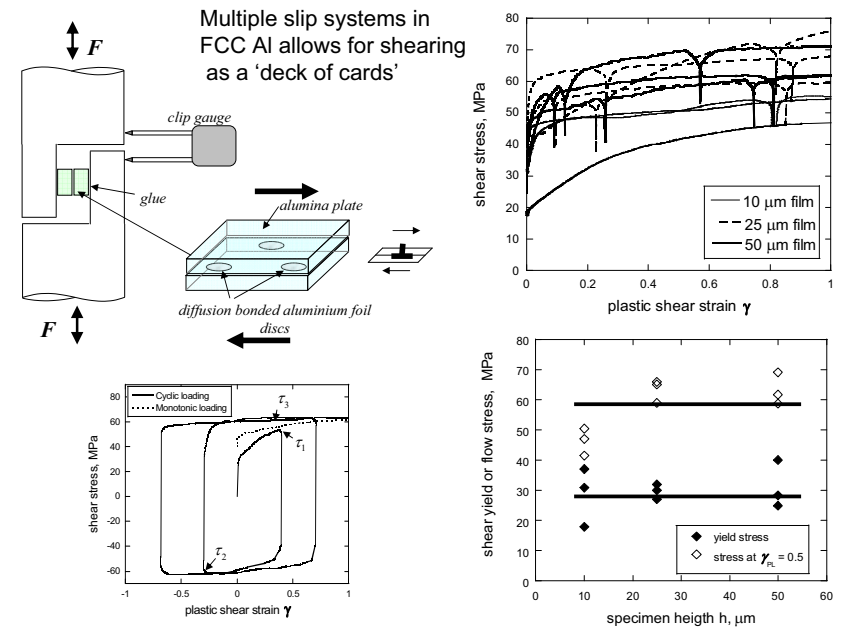
$$s_i^{(\alpha)} = \cos \varphi^{(\alpha)} e_i^{(1)} + \sin \varphi^{(\alpha)} e_i^{(2)}$$

Unit normal of the slip planes

$$m_i^{(\alpha)} = -\sin \varphi^{(\alpha)} e_i^{(1)} + \cos \varphi^{(\alpha)} e_i^{(2)}$$

□ Plastic response for interface and bulk is the same

## Possible size effects in a sandwiched aluminium film under shear



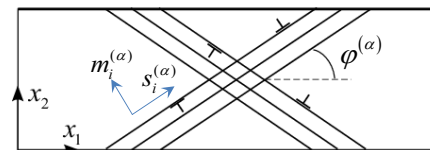
# Strain Gradient Crystal Plasticity Theory

## Kinematics

$$\dot{\epsilon}_{ij} = (\dot{u}_{i,j})_{\text{symm}} = \dot{\epsilon}_{ij}^e + \dot{\epsilon}_{ij}^p, \quad \dot{\epsilon}_{ij}^p = \sum_{\alpha} \dot{\gamma}_p^{(\alpha)} \mu_{ij}^{(\alpha)}$$

Schmid orientation tensor:

$$\mu_{ij}^{(\alpha)} = (s_i^{(\alpha)} m_j^{(\alpha)} + m_j^{(\alpha)} s_i^{(\alpha)}) / 2$$



Slip direction vector

$$s_i^{(\alpha)} = \cos \varphi^{(\alpha)} e_i^{(1)} + \sin \varphi^{(\alpha)} e_i^{(2)}$$

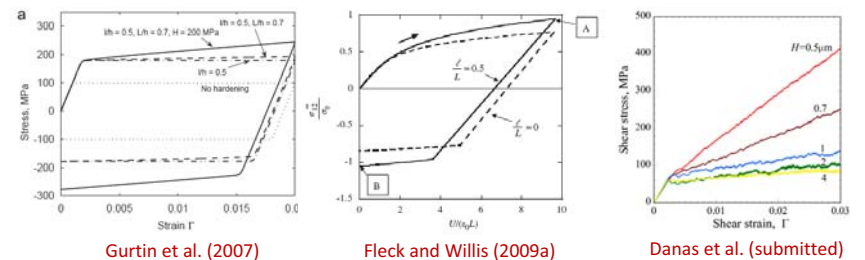
Unit normal of the slip planes

$$m_i^{(\alpha)} = -\sin \varphi^{(\alpha)} e_i^{(1)} + \cos \varphi^{(\alpha)} e_i^{(2)}$$

Gurtin (2002), Borg (2007), Fleck and Willis (2009a)

# Do sheared single crystals exhibit size effects?

When a single crystal is under simple shear theoretical results predict strong size effects, assuming full plastic constraint at the interface...



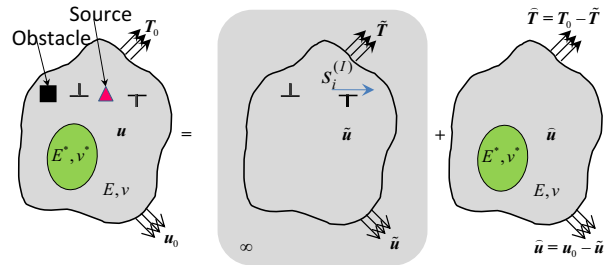
Recent (unpublished) experimental results by Tagarielli and Fleck (2009?) indicate **negligible** size effects upon shearing of single aluminium crystals ???



One possible explanation: manufacture of the sandwich specimen (e.g., the joining of two dissimilar solids by diffusion bonding) generates an **interface of finite thickness** with an internal structure that is more amorphous than that of the bulk and consequently more **compliant**.



## Discrete Dislocation framework – Plane Strain



At a given instant in time:  $u_i = \tilde{u}_i + \hat{u}_i, \quad \varepsilon_{ij} = \tilde{\varepsilon}_{ij} + \hat{\varepsilon}_{ij}, \quad \sigma_{ij} = \tilde{\sigma}_{ij} + \hat{\sigma}_{ij}$

(~) fields – sum of the singular equilibrium fields of the individual dislocations

$$\tilde{u}_i = \sum_{J=1}^{N_d} \tilde{u}_i^{(J)}, \quad \tilde{\varepsilon}_{ij} = \sum_{J=1}^{N_d} \tilde{\varepsilon}_{ij}^{(J)}, \quad \tilde{\sigma}_{ij} = \sum_{J=1}^{N_d} \tilde{\sigma}_{ij}^{(J)}, \quad \tilde{\sigma}_{ij}^{(J)} = 0$$

(^) fields – image non-singular fields that correct for the boundary conditions

Van der Giessen and Needleman (1995), Deshpande and coworkers (2001, 2002, 2005, 2008)

## Strain Gradient Crystal Plasticity Theory

### Principle of Virtual Work

Independent variables:  $\dot{u}_i, \dot{\gamma}_p^{(\alpha)}, \dot{\gamma}_{p,i}^{(\alpha)}$  → Conjugate variables:  $\sigma_{ij}, q^{(\alpha)}, \tau_i^{(\alpha)}$

$$\int_V \left( \sigma_{ij} \delta \dot{\varepsilon}_{ij} + \sum_{\alpha} \left( q^{(\alpha)} - \sigma_{ij} \mu_{ij}^{(\alpha)} \right) \delta \dot{\gamma}_p^{(\alpha)} + \sum_{\alpha} \tau_i^{(\alpha)} \delta \dot{\gamma}_{p,i}^{(\alpha)} \right) dV = \int_S \left( T_i \delta u_i + \sum_{\alpha} t^{(\alpha)} \delta \dot{\gamma}_p^{(\alpha)} \right) dS$$

Field equations:  $\sigma_{ij,j} = 0, \quad q^{(\alpha)} - \tau_{i,i}^{(\alpha)} = \sigma_{ij} \mu_{ij}^{(\alpha)}$

Boundary Tractions:  $T_i = \sigma_{ij} n_j, \quad t^{(\alpha)} = \tau_i^{(\alpha)} n_i \quad \text{on } S_t$

Displacement BC:  $u = u_0, \quad \dot{\gamma}_p^{(\alpha)} = \dot{\gamma}_p^{(\alpha)0} \quad \text{on } S_u$

Gurtin (2002), Borg (2007), Fleck and Willis (2009a)

## DD short range interaction and motion

Dislocation dipoles with Burgers vector  $b$  are nucleated at randomly distributed point sources (Frank-Read) when the resolved shear stress takes a value  $\tau_{nuc}$ .

The glide component of the Peach-Koehler force, and dislocation motion:

$$f^{(l)} = s_i^{(l)} \left[ \tilde{\sigma}_{ij} + \sum_{J \neq l} \tilde{\sigma}_{ij}^{(J)} \right] b_j^{(l)}, \quad v^{(l)} = f^{(l)} / B_{drag}$$

Annihilation of two opposite signed dislocations on a slip plane occurs when in a material dependent critical annihilation distance  $L_e$ .

The obstacles to dislocation motion are randomly distributed points on the slip planes. An obstacle releases a pinned dislocation when the Peach-Koehler force on the obstacle exceeds  $\tau_{obs} b$ .

## Strain Gradient Crystal Plasticity Theory

### Constitutive equations

$$U(\varepsilon_{ij}^e, \gamma_p^{(\alpha)}, \gamma_{p,i}^{(\alpha)}) = U_e(\varepsilon_{ij}^e) + \sum_{\alpha} U_p^{(\alpha)}(\gamma_p^{(\alpha)}, \gamma_{p,i}^{(\alpha)}) \Rightarrow \sigma_{ij} = \partial U_e / \partial \varepsilon_{ij}^e$$

$$q^{(\alpha)} = q^{E(\alpha)} + q^{D(\alpha)}, \quad \tau_i^{(\alpha)} = \tau_i^{E(\alpha)} + \tau_i^{D(\alpha)}$$

#### Energetic terms

$$\gamma_e^{(\alpha)} = \left( |\gamma_p^{(\alpha)}|^2 + |L \gamma_{p,i}^{(\alpha)} s_i^{(\alpha)}|^2 \right)^{1/2}$$

energetic length scale

$$\text{defect energy: } U_p^{(\alpha)} = \frac{G}{2} \left( \gamma_e^{(\alpha)} \right)^2$$

$$q^{E(\alpha)} = \partial U_p^{(\alpha)} / \partial \gamma_p^{(\alpha)}$$

$$\tau_i^{E(\alpha)} = \partial U_p^{(\alpha)} / \partial \gamma_{p,i}^{(\alpha)}$$

#### Dissipative terms

$$\dot{\gamma}_e^{(\alpha)} = \left( |\dot{\gamma}_p^{(\alpha)}|^2 + |l \dot{\gamma}_{p,i}^{(\alpha)} s_i^{(\alpha)}|^2 \right)^{1/2}$$

dissipative length scale

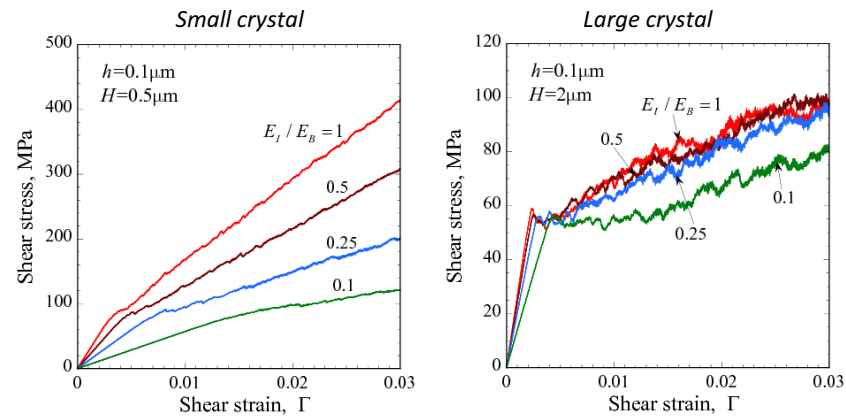
$$\text{dissipation potential: } \phi^{(\alpha)} = \frac{\sigma_y \dot{\gamma}_0}{m+1} \left( \frac{\dot{\gamma}_e^{(\alpha)}}{\dot{\gamma}_0} \right)^{m+1}$$

$$q^{D(\alpha)} = \partial \phi^{(\alpha)} / \partial \dot{\gamma}_p^{(\alpha)}$$

$$\tau_i^{D(\alpha)} = \partial \phi^{(\alpha)} / \partial \dot{\gamma}_{p,i}^{(\alpha)}$$

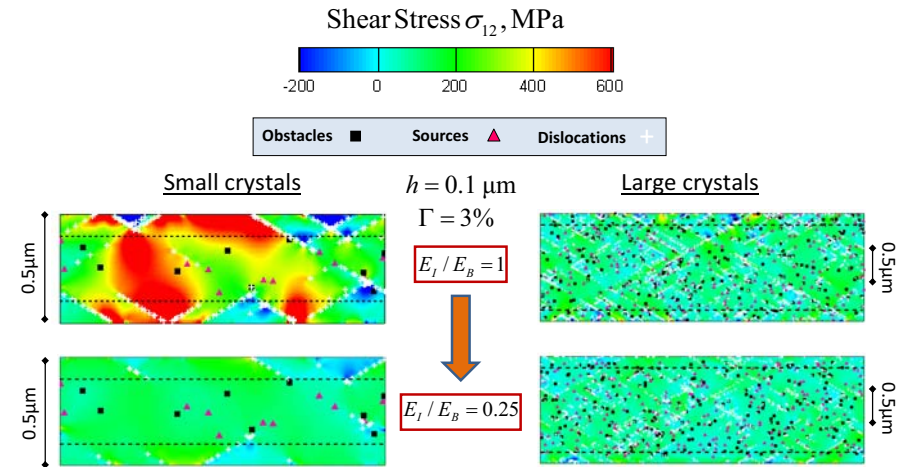
## DD Shear Stress – Shear Strain results

Sensitivity analysis of the Young's moduli ratio  $E_I / E_B$



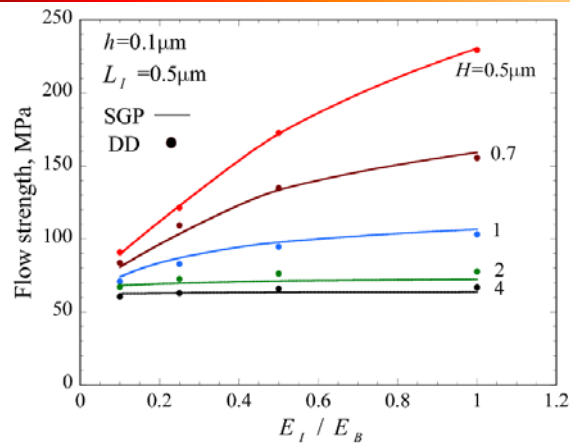
Result: Size effects significantly reduce as interfaces become more compliant!

## Contours of Shear Stress from DD calculations



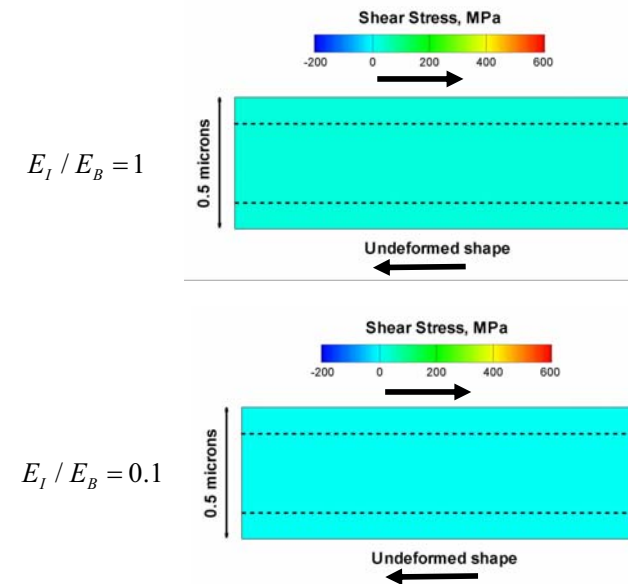
- Higher stresses develop in thinner films due to the back stress generated by dislocation pile-ups inhibiting nucleation throughout the film

## SGP vs. DD flow strength collective results



In the SGP calculation we use the length scales:  $l_I = l_B = L_B = 0.25 \mu\text{m}$ ,  $L_I = 2 L_B$

The flow strength is defined as the average shear stress over the interval  $1\% \leq \Gamma \leq 2\%$



## Concluding remarks

---

- It is now generally accepted that size effects exist in plasticity, although there remains debate as to the cause. A number of continuum theories have emerged, and are in broad agreement with discrete dislocation simulations.
- The constitutive response of an interface remains an open issue, and critical experiments are still needed to give insight into the flow resistance by an interface.